Published in final edited form as:
Nat Chem Biol. 2010 January ; 6(1): 25–33. doi:10.1038/nchembio.275.

Reduced Histone Deacetylase 7 Activity Restores Function to Misfolded CFTR in Cystic Fibrosis

Darren M. Hutt[1,*], **David Herman**[2,*], **Ana P. C. Rodrigues**[3], **Sabrina Noel**[4], **Joseph M. Pilewski**[5], **Jeanne Matteson**[1], **Ben Hoch**[2], **Wendy Kellner**[1], **Jeffery W. Kelly**[6,7], **Andre Schmidt**[8], **Philip J. Thomas**[8], **Yoshihiro Matsumura**[9], **William R. Skach**[9], **Martina Gentzsch**[10], **John R. Riordan**[11], **Eric J. Sorscher**[12], **Tsukasa Okiyoneda**[13], **Gergely L. Lukacs**[13], **Raymond A. Frizzell**[4], **Gerard Manning**[3], **Joel M. Gottesfeld**[2], and **William E. Balch**[1,2,14,15,#]

[1]Departments of Cell Biology at The Scripps Research Institute, 10550 North Torrey Pines Rd, La Jolla, CA, 92037 USA

[2]Department of Molecular Biology at The Scripps Research Institute, 10550 North Torrey Pines Rd, La Jolla, CA, 92037 USA

[15]Department of Chemical Physiology at The Scripps Research Institute, 10550 North Torrey Pines Rd, La Jolla, CA, 92037 USA

[14]The Institute for Childhood and Neglected Diseases at The Scripps Research Institute, 10550 North Torrey Pines Rd, La Jolla, CA, 92037 USA

[6]Department of Chemistry at The Scripps Research Institute, 10550 North Torrey Pines Rd, La Jolla, CA, 92037 USA

[7]Skaggs Institute of Chemical Biology at The Scripps Research Institute at The Scripps Research Institute, 10550 North Torrey Pines Rd, La Jolla, CA, 92037 USA

[3]Resave Newman Center for Bioinformatics, Salk Institute for Biological Studies, La Jolla, CA, 92037 USA

[4]Department of Cell Biology and Physiology, University of Pittsburgh School of Medicine, Pittsburgh, PA 15261

[5]Division of Pulmonary, Allergy and Critical Care Medicine, University of Pittsburgh School of Medicine, Pittsburgh, PA 15261

[8]Molecular Biophysics, University of Texas Southwestern Medical Center, 6001 Forest Park Lane, Dallas, TX 75390

[9]Department of Biochemistry and Molecular Biology, Oregon Health and Sciences University, Portland, OR 97239

[10]Department of Cell and Developmental Biology, University of North Carolina, Chapel Hill, NC 27599

[11]Department of Biochemistry and Biophysics, University of North Carolina, Chapel Hill, NC 27510

[#] To whom correspondence should be directed: webalch@scripps.edu.
[*]Contributed equally

Competing Financial Interests: No competing financial interests.

[12]Department of Cell Biology and Physiology, University of Alabama at Birmingham, Birmingham, AL 35294

[13]Department of Physiology, McGill University, Montreal, QC, H3G1Y6 Canada.

Abstract

Chemical modulation of histone deacetylase (HDAC) activity by HDAC inhibitors (HDACi) is an increasingly important approach to modify the etiology of human disease. Loss-of-function diseases arise as a consequence of protein misfolding and degradation leading to system failures. The ΔF508 mutation in cystic fibrosis transmembrane conductance regulator (CFTR) results in the absence of the cell surface chloride channel and a loss of airway hydration, leading to premature lung failure and reduced lifespan responsible for cystic fibrosis (CF). We now show that the HDACi suberoylanilide hydroxamic acid (SAHA) restores surface channel activity in human primary airway epithelia to levels that are 28% of wild-type CFTR. Biological silencing of all known class I and II HDACs reveals that HDAC7 plays a central role in restoration of ΔF508 function. We suggest that the tunable capacity of HDACs can be manipulated by chemical biology to counter the onset of CF and other human misfolding disorders.

Cystic Fibrosis (CF) is caused by mutations in the CFTR gene1, which encodes a multi-membrane spanning epithelial chloride channel. Ninety percent of patients have a deletion of Phe 508 (ΔF508) on at least one allele. This mutation results in disruption of the energetics of the protein fold2 leading to efficient degradation of CFTR in the endoplasmic reticulum (ER). The loss of a functional CFTR channel at the plasma membrane disrupts ionic homeostasis (Cl^-, Na^+, HCO_3^-) and airway surface hydration leading to reduced lung function1. Reduced periciliary liquid volume and increased mucus viscosity impede mucociliary clearance resulting in chronic infection and inflammation, phenotypic hallmarks of CF disease[3]. In addition to respiratory dysfunction, ΔF508 also impacts the normal function of additional organs (pancreas, intestine, gall bladder), suggesting that the loss-of-function impacts multiple downstream pathways that will require correction.

CF and other maladies of protein misfolding, including lysosomal storage diseases, type II diabetes, and cardiovascular and neurological diseases, arise as a result of an imbalance in the capacity of the protein homeostasis (proteostasis) environment to handle the reduced energetic stability of misfolded, mutated proteins that are critical for normal physiology[4-6]. The cellular proteomic and metabolic environment is highly adaptable, and responds to stress and disease through numerous signaling pathways that include, among others, the unfolded protein response (UPR) and heat-shock response (HSR). The latter respond to misfolding and/or aggregation of proteins by altering the transcriptional and post-translational regulation of synthesis, folding and trafficking components to restore function to the protein fold as well as cell, tissue and host physiology[4,7].

Histone acetyl transferase (HATs) and deacetylases (HDACs) are known to modulate transcriptional events that alter cellular function during development and in response to environmental changes[8,9]. These enzymes not only mediate post-translational acetylation and deacetylation reactions, respectively, of histones, but of transcription factors and other cytosolic factors such as the chaperone Hsp9010. The human genome encodes 18 HDACs, belonging to four distinct structural classes9. Recent studies have suggested that modification of HDAC activity using chemical inhibitors can have substantial beneficial effects in, for example, mouse models of type II diabetes[11], airway inflammation[12] and rheumatoid arthritis[13], yet the HDACi in question exhibits limited specificity towards individual HDAC family members. Although it is not known if HDACi provide benefit by

targeting a single or multiple HDAC, siRNA silencing of individual HDACs strongly implicate specific roles for distinct family members in human health and disease[14].

Herein, we demonstrate restoration of ΔF508-CFTR function in primary lung epithelial cells through an HDACi-sensitive mechanism(s). Furthermore, we show that by siRNA-mediated silencing of the human lung-enriched HDAC7 [15] we can achieve a striking increase in stabilization, trafficking and activity of ΔF508 cell surface chloride channel activity. We propose that the mechanism by which HDAC inhibition may benefit CF and perhaps other misfolding diseases involves the capacity of altered acetylation states to influence the epigenome and readjust cellular physiology to restore function to misfolded proteins.

RESULTS

Treatment with HDAC inhibitors improves ΔF508 stability and trafficking

We have previously shown that CFTR folding requires Hsp9016, an HDAC sensitive chaperone that is inhibited by acetylation10,[17]. We, therefore, sought to assess the effect of a panel of small molecule HDAC inhibitors (HDACi) spanning various chemical scaffolds on the trafficking and function of ΔF508 at physiological temperature (37°C) in a bronchial epithelial cell line (CFBE41o-)[18] that expresses ΔF508. This cell line is used for all experiments unless otherwise indicated.

Transport of CFTR from the ER to the cell surface can be monitored by a change in migration on SDS-PAGE. ER-acquired N-linked oligosaccharides (Fig 1a, upper panel band B) are processed during trafficking through the Golgi to generate the slower migrating, band C glycoform as shown for the thermal-sensitive ΔF508 cultured at reduced temperature (30°C) (Fig. 1a, upper panel (lane 1)). Using maximal stimulating concentrations of trichostatin A (TSA) (**1**), suberoylanilide hydroxamic acid (SAHA) (**2**), Scriptaid (**3**) and MS-275 (**4**) (Fig. 1b **and** Supplemental Fig. S1), HDACis that yielded correction of ΔF508 trafficking (Supplemental Fig. S2a), we observed that each compound increased ΔF508 mRNA (Supplemental Fig. S2b) as well as total CFTR protein levels including the accumulation of the band C cell surface glycoform relative to the vehicle treated cells (Fig. 1a, **upper panel; quantitated in lower panel**). The increased protein expression in response to these HDACi was potently blocked by simultaneous treatment with actinomycin D (**5**) (Supplemental Fig. S1), an inhibitor of transcription (Supplemental Fig. S2c). These data suggest that the effect of HDACs on ΔF508 is primarily through transcriptional events.

In order to address whether the observed effect was the result of altered expression of ΔF508 or altered expression of proteins that may regulate ΔF508 biogenesis and trafficking, we monitored the early effects of the HDACi, SAHA. We observed an increased band B level as early as 1 h (Fig. 1c, **upper panel; quantitated in lower panel**), as well as the appearance of band C after 4 h (Fig. 1c, inset) events that precede the increased ΔF508 transcription, which is first observed at 8 h following SAHA treatment (Supplemental Fig. S2d). This early onset rescue coincides with epigenetic modification(s), as evidenced by the rapid hyperacetylation of histone H3 (Fig. 1c, upper panel), suggesting the existence of a subset of genes, highly responsive to HDAC inhibition, which act alone or in concert to mediate the observed increased stability and trafficking of ΔF508. Consistent with this conclusion, SAHA has no effect on the expression of CFTR in an *in vitro* translation assay (Supplemental Fig. S3a) nor does it stabilize the native state of recombinant NBD1 lacking Phe 508 (Supplemental Fig. S3b). These data support the conclusion that SAHA is not acting directly on ΔF508, but rather on accessory factors mediating its biogenesis and trafficking.

Given the elevated expression of bands B and C in response to HDACi (Fig. 1a), we were interested in whether the appearance of band C reflected 'leak' from the ER that was simply proportional to the larger pool of band B that exited at a similar rate to vehicle-treated cells, or a consequence of an increased rate of trafficking. The ratio of band C to band B can be used to indicate the level of post-ER glycoforms of CFTR relative to the ER pool. In vehicle treated cells the C/B ratio was 0.07, a value reflecting the nearly negligible levels of band C observed at steady state in the CFBE41o- cells. TSA, SAHA and Scriptaid yielded a 3-fold increase in the C/B ratio, which is comparable to low temperature rescue (Fig. 1a, lower panel), while MS-275 treatment yielded a 1.4-fold increase (Fig. 1a, lower panel). These results support the conclusion that the increased ER load of ΔF508 CFTR is not solely responsible for the increased trafficking.

To account for the increased appearance of band C in response to HDACi, we performed a pulse-chase analysis of ΔF508 following a 24 h treatment with 5 μM SAHA. In control cells, band B exhibited a $T_{1/2}$ of 1 h (Fig. 1d, upper panel) with exponential decay kinetics, consistent with its published half-life[19]. This increased ~2-fold after treatment with SAHA, which showed linear decay kinetics (Fig. 1d, upper panel), supporting the conclusion that ΔF508-CFTR exhibits a significant increased stability following HDACi treatment. We also tested the effect of SAHA on an analogous cell line (HBE41o-) that expresses wild-type (WT) CFTR. Interestingly, although we did not observe any significant decay in total WT CFTR over the 3 h chase period, we did observe a significant acceleration in the rate of maturation of CFTR to the band C glycoform in response to a 24 h treatment with 5 μM SAHA (Fig 1d, lower panel). These data suggest that SAHA not only mediates an increased stability of ΔF508, but can improve trafficking of even wild-type CFTR to the cell surface.

We did not observe major changes of HSR chaperone proteins Hsp90, Hsc70, Hop, and p23, previously shown to facilitate ΔF508-CFTR maturation[16], or markers of UPR or HSR including BiP and Hsp70, respectively (see Supplemental Fig. S4 **for Western blots),** in response to HDACi (Fig. 1a). Therefore, these HDACi do not appear to be working through signaling pathways that typically respond to cellular protein misfolding. We also did not observe correction of the trafficking defect associated with the ER-restricted mutant of glucocerebrosidase, L444P, which causes Gaucher's disease and is sensitive to UPR induction (Supplemental Fig. S5). This suggests that the SAHA-mediated correction of ΔF508 trafficking is not the result of a more general effect on the up-regulation of chaperone components characteristic of UPR or HSR responsive pathways.

In order to establish the subcellular localization of the band C pool, we assessed surface expression of ΔF508 using immunofluorescence in BHK cells stably expressing an extracellular loop HA-tagged ΔF508 ($\Delta F508^{extope}$)[20]. SAHA, Scriptaid and MS-275 all exhibited increased plasma membrane localized $\Delta F508^{extope}$ relative to vehicle treated cells (Fig. 1e). SAHA yielded a nearly 5-fold increase relative to that seen with known CFTR correctors found in the CFTR modulator library (http://cftrfolding.org/CFFTReagents.htm) (Fig. 1d). Moreover, SAHA exhibited synergy with corrector C3 (**6**) (Supplemental Fig. S1), that promotes a low level of ΔF508 correction (Fig. 1d). An identical response was observed using an independent assay to examine cell surface stability in IB3 cells expressing $\Delta F508^{extope}$ (GL, data not shown). In contrast, inhibitors of class III HDACs (sirtuins) had no effect on restoration of ΔF508 activity (Supplemental Fig. S6). Collectively, these data demonstrate that treatment with inhibitors of class I, II and IV HDACs results in increased stability and trafficking of ΔF508 to the cell surface.

Increased stability and trafficking of ΔF508 in response to chronic, low dose SAHA

Given the robust effect of SAHA on ΔF508 stability and trafficking in response to acute treatment (5 μM for 24 h), we examined whether a lower, prolonged chronic dosing

schedule (1 μM every 24 h) could sustain or enhance ΔF508 correction. Intriguingly, we observed a time-dependent increase in both total ΔF508 expression and the level of band C (Fig. 2a, **left panel; quantitated in right panel**) as well as a strong increase in the C/B ratio after 6-8 days (Fig. 2a, right panel (inset)) equivalent to that observed with acute treatment. To determine if the low-dose protocol resulted in a stabilizing influence that would persist after drug withdrawal, we monitored ΔF508 following washout of SAHA after an initial treatment period of 1, 5 or 10 days with 1 μM. Pretreatment for 5 days resulted in complete stabilization of band C in the first 24 h period following SAHA removal, a result not observed with the 1-day pretreatment at the same dose (Fig. 2b). Using a similar regimen, we also observed a sustained surface density for 24 h following drug withdrawal in a stable cell line (CFBE-L-ΔF508) expressing ΔF508 containing an epitope-tag in the extracellular domain (Fig. 2c). A 10-day pretreatment with 1 μM did not lead to a further stabilization of band C following SAHA withdrawal. We conclude that increased ΔF508 stability is favored by a low dosing regime that achieves a level of ΔF508 expression that is managed by integration of folding in the ER with trafficking to the cell surface.

Rescue ofΔF508 chloride channel activity by HDACi

The appearance of band C and its surface localization suggest that HDACi treatment may lead to recovery of channel activity. Therefore, we examined the effect of HDACi on cAMP-stimulated iodide efflux in ΔF508 expressing CFBE41o- cells. Treatment with an acute dose of TSA, SAHA or Scriptaid (Fig. 1a) yielded a ~2.5 fold stimulation of efflux relative to the ~4-fold increase observed for temperature rescued (30°C) or wild-type CFTR (Fig. 3a). A measurement of short circuit currents in CFBE41o- monolayers treated with SAHA (Fig. 3b; Supplemental **Fig. S7b**) or TSA (Supplemental Fig. S7a) yielded identical results. Curiously, treatment with 5 μM MS-275, which showed a similar increase in total ΔF508 to that seen with 1 μM Scriptaid based on immunoblotting as well as a rescue of trafficking to band C (Fig. 1a) and surface labeling (Fig. 1e), exhibited no significant stimulation of iodide efflux relative to DMSO treated controls (Fig. 3a). Thus, rescue of ΔF508 trafficking, as seen by the appearance of band C and surface labeling, does not necessarily reflect acquisition of channel activity. This raises the possibility that functional correction of ΔF508 requires at least three independent events including (1) altered ER stability, (2) altered ΔF508 CFTR trafficking, as observed with all HDACi tested, and (3) regulation of channel activity, as observed following TSA, Scriptaid and SAHA treatment.

To establish a causal basis for the differential effect of these HDACi in promoting stability, trafficking and function of ΔF508, all compounds were tested for their ability to inhibit recombinant HDACs in an *in vitro* deacetylation assay (Supplemental Table S1). TSA, SAHA and Scriptaid appear to be pan HDAC inhibitors (but see21) whereas MS-275 is largely selective for Class I HDACs. The ability of MS-275 to rescue stability and trafficking, but not function, implies that inhibition of class II HDACs evokes an additional activity(s) necessary for channel function of ΔF508 at the cell surface.

Silencing of HDAC1 and 7 enhances ΔF508 stability and trafficking

To begin to address the mechanism of HDACi action, we examine the effect of siRNA silencing of HDACs in CFBE41o- cells, in order to establish which of the isoforms were responsible for correction of the ΔF508-CFTR trafficking defect. There are 18 human HDACs that cluster into four classes by homology[22,23]: Zn^{2+}-dependent class I (HDAC1, 2, 3 and 8), II (4-7, 9 and 10) and IV (HDAC11) enzymes, and the NAD^{+}-dependent class III (sirtuins), which are insensitive to the inhibitors tested above[23,24]. Silencing of HDACs 2 and 3 (Supplemental Fig. S8a) caused a 2.5- and 1.5-fold increase in ΔF508-CFTR mRNA (Supplemental Fig. S8b), respectively, as well as an ~5-fold increase in total ΔF508 protein (Fig. 4a, upper panel (compare lanes 2,4,5); quantitated in the lower panel). Here, ΔF508

was recovered primarily in the *band B* glycoform (Fig. 4a (lanes 4,5)). As expected[16], silencing of HDAC6 (Supplemental Fig. S8a), which would lead to accumulation of the inactive, acetylated Hsp90, destabilized ΔF508 (Fig. 4a, upper panel **(**lane 8)). By contrast, silencing of HDACs 1 or 7 (Fig 4b and Supplemental Fig. S8a) resulted in a 9- and 15-fold increase in total ΔF508-CFTR protein, respectively (Fig. 4a, upper panel (compare lanes 2,3,9); quantitated in the lower panel). Importantly, both siHDAC1 and siHDAC7 rescued ΔF508 trafficking as indicated by the appearance of band C (Fig. 4a, upper panel (lanes 3,9); lower panel).

An analysis of the C/B ratio suggest that silencing of individual HDACs can result in an increased rate of trafficking as shown above for various HDACi. In cells transfected with scrambled siRNA (siScr), the C/B ratio was 0.05 (Fig. 4a, lower panel) showing that very little ΔF508 escapes the ER. Despite an increased protein expression following silencing of HDACs 2 or 3, the C/B ratio remained unaltered (Fig. 4a, lower panel). By contrast, silencing of HDAC1 or HDAC7 resulted in a 5- and 16-fold increase in C/B ratio, respectively (Fig. 4a, lower panel). Thus, silencing of select HDACs, particularly HDAC7, supports increased stabilization and trafficking of ΔF508-CFTR. This is consistent with the pulse-chase analysis in CFBE41o- cells following siHDAC7 treatment, which revealed a 2-fold increase in ΔF508 stability (Fig. 4c). Because no substantial change was observed in the expression of UPR and HSR components (see Supplemental Fig. S9 **for Western blots**) in response to siHDAC7 (Fig. 4a, upper panel), the observed correction appears to operate independently of ER and cytosolic stress signaling pathways.

Correction of ΔF508 CFTR activity by silencing of HDAC7

To address more thoroughly the role of individual HDACs active in ΔF508 rescue, we examined the effects of the siHDAC1 and 7 on ΔF508 channel activity in CFBE41o-cells. siHDAC1 induced a 1.4-fold stimulation of iodide efflux that was not observed with siRNAs to other Class I members (Fig. 4d). In contrast, silencing of HDAC7 exhibited a 3.6-fold stimulation of cAMP-mediated iodide efflux comparable to 30°C efflux (Fig. 4d). This activity was blocked by treatment with the CFTR channel inhibitor CFInh-172 (**7**) (Supplemental Fig. S1) (Fig. 4d), indicating that iodide efflux occurs via a corrected ΔF508 channel. The observed cAMP-mediated iodide efflux seen with siHDAC7 treatment in CFBE41o- is greater than that seen with general HDACi ($p < 0.01$), suggesting that HDAC7 offers fewer off-target effects that could be detrimental to ΔF508 stability, trafficking and activity.

HDACi rescues human primary bronchial epithelial airway cells homozygous for ΔF508

Given that technical limits impede our ability to silence HDAC7 in primary bronchial epithelial cells homozygous for ΔF508 (ΔF/ΔF-HBE) obtained from patients, we examined the effect of SAHA, the most efficacious of the HDACi tested, on ΔF508 stability, trafficking and transepithelial anion secretion in ΔF/ΔF-HBE. Relative to control, acute SAHA treatment (10 μM for 24 h) resulted in a ~6-fold stimulation of channel activity in response to forskolin alone, with a significant additive effect upon addition of genistein, a well-characterized CFTR channel potentiator (Fig. 5a; Supplemental Fig. S7c). Stimulation was nearly completely inhibited by CFTRInh-172[25] (Fig. 5a; Supplemental **Fig. S7c**). Similar effects were observed from primary lung cells derived from multiple patients (RF/SN, data not shown). The average channel activity stimulated by forskolin (**8**) (Supplemental Fig. S1) and genistein (**9**) (Supplemental Fig. S1) is 3.7 ± 0.8 μA/cm^2, representing a level of correction of 15.0 ± 5.4 % of the channel activity seen in wild-type CFTR expressing cells (23.1 ± 5.8 μA/cm^2). The ability to detect significant ΔF508 channel activity following acute treatment with forskolin alone indicates a substantial alteration in ΔF508 channel properties *in vivo* in response to HDACi.

Given the impact of a chronic low dose SAHA treatment on ΔF508 function in the CFBE41o-cell line (Fig. 2a), its effect was examined on primary ΔF/ΔF-HBE cells. Cells exposed to 1 μM SAHA for 4, 6 and 8 days exhibited a significant increase in short circuit currents (ΔIsc) relative to DMSO controls (Fig. 5b). Following 8 days of treatment, cells exhibited a ΔIsc of 6.5 ± 1.0 μA/cm^2, representing a restoration of channel activity to 28.0 ± 8.3 % of the wild-type level (23.1 ± 5.8 μA/cm^2) (Fig. 5b), nearly 2-fold larger than that observed by the acute treatment regime. Longer dosing regimes did not result in further increased channel activity (RF/SN, data not shown). Interestingly, the activity seen with a chronic 8 day application of 1 μM SAHA was fully sustained for up to 2 days following withdrawal of the compound from the culture media (Fig. 5c), a result that is not observed following acute treatment (RF/SN, data not shown). Although we observed a progressive decay in the channel activity with increasing time of withdrawal of SAHA, a statistically significant increase in channel activity was maintained for up to 8 days post-withdrawal as compared to untreated cells (Fig. 5c).

Immunoblot analysis of lysates from these ΔF/ΔF-HBE cells treated with 1 μM SAHA for 8 days showed a ~2-fold increase in band B. Thus, unlike the CFBE41o- cell line expressing ΔF508 from a SAHA responsive CMV promoter, SAHA had only a minimal impact on CFTR expression from the native promoter, emphasizing the importance of non-CFTR biological pathways in correction. Compared to untreated cells, we observed a progressive accumulation of band C (Fig. 5d) to a level representing ~75% of that seen in non-CF HBE cells (Fig. 5e). Intriguingly, based on immunoblotting, primary ΔF/ΔF-HBE exposed to the low dose SAHA regime exhibited a sustained pool of band C following 4 days of SAHA withdrawal (Fig. 5d), a result consistent with the observed sustained increase in channel activity (Fig. 5c).

To address whether the band C observed in Western blots corresponded to a significant cell surface apical pool in polarized cells, primary HBE cells were infected with adenovirus expressing ΔF508^{extope}. ΔF508 CFTR localized to the apical surface in response to all HDACi tested, with the strongest localization observed with SAHA (Fig. 5f). Thus, patient ΔF/ΔF-HBE recapitulate a high level of responsiveness to SAHA using multiple independent criteria.

Network analysis reveals a shift in the CFTR interaction pathways favoring correction

We used gene expression profiling to search for transcriptional targets that might mediate the siHDAC7 effect on stability, trafficking and activity of ΔF508-CFTR. Genes whose expression was changed by siHDAC7 (Supplemental Fig. S10 **and** Supplemental Table S2) were significantly enriched (p = 8.9e-8) in CFTR-interacting proteins found in the GeneGo CF platform[26] (Fig. 6a), a literature curated summary of known physical interactions and pathways involved in CF. Here, the HDAC7-modulated CFTR-interacting gene set contains 41 genes, much larger than the 19 genes expect by random chance (p<0.5) and larger than the 28 genes required for statistical significance (at p<0.01). Thus, HDAC7 appears to alter the expression of genes linked to multiple distinct CFTR pathways affecting ΔF508-CFTR including its folding and maturation, trafficking, and channel activation (Fig. 6a, Supplemental Fig. S10). For example, we observed increased expression of BAG227, a known Hsc/Hsp70 repressor that protects CFTR from degradation and that is likely linked through Hsc/Hsp70 to the Hsp90 system required for folding16. siHDAC7 also up-regulated Sec31 and Sar1b, components involved in COPII coat complex formation previously shown to be critical for CFTR export in human cells[28,29]. This latter observation was confirmed by chromosomal immunoprecipitation (ChIP) were increased levels of acetylated histone H3 and polymerase II were found at the Sar1b promoter following SAHA treatment of CFBE41o-cells (Supplemental Fig. S11). In contrast, we observed an increase in the expression of both Sec61 and Derlin1, previously shown to mediate the retrotranslocation

and degradation of misfolded ΔF508 [27]. Although at first confounding, this observation raises the possibility that the cell retains the ability to dispose of elevated misfolded CFTR, an interpretation consistent with the absence of UPR or HSR response following either HDACi or siHDAC7 treatment. The combined changes would be predicted to favor increased ER stability of a folded form of ΔF508 that is recognized for trafficking from the ER[30]

Post-ER components that would promote cell surface stability and activity include a decreased expression of TC10, disabled homolog 2 (DAB2) and AP2 complex. These components affect CFTR recycling through the endosomal system and their reduced expression would favor cell surface localization[31]. Moreover, down-regulation of the t-SNARE, SNAP 23, a known inhibitor of CFTR channel activity, as well as up-regulation of filamin B, shown to stabilize surface membrane localized CFTR would favor cell surface stability and increased channel activity31. In addition, altered kinase signaling pathways (Fig. 6a; Supplemental Fig. 10) may more effectively modulate defective channel gating, a feature characteristic of reduced temperature-rescued ΔF508 when re-incubated at 37°C. While we cannot necessarily correlate every change in expression with the final successful outcome leading to increase ΔF508 channel activity, it is apparent that HDAC7-sensitive pathways can be used to manage the destabilizing effect of the ΔF508 to increase folding and stability in the ER, and trafficking and activity at the cell surface.

In summary, changes at multiple levels of the network of interactions facilitating CFTR folding and function (Fig. 6b) may contribute stepwise to the resolution of channel deficiency at the cell surface and would be expected to significantly impact the etiology of CF disease.

DISCUSSION

Herein we show that the trafficking defect associated with ΔF508-CFTR can be overcome in response to inhibition of HDAC activity. Although the classical cycle of acetylation/deacetylation mediated by HATs and HDACs respectively, has been best described for histones, it has been shown that numerous other proteins are regulated by post-translational acetylation and therefore suggests two possible mechanisms by which inhibition of HDACs may correct trafficking of ΔF508. In the first instance, HDACis may alter the acetylation state of histones influencing the epigenome, which in turn alters the transcriptional level of a number of CFTR related genes that either act alone or in concert to overcome the trafficking block associated with ΔF508. Alternatively, HDACi's could modulate the activity of a subset of proteins via post-translational acetylation, as has been shown for numerous proteins, including the chaperone Hsp90[10], the end result being correction of function. Since we were unable to observe either an increase in stability or trafficking with SAHA in the absence of *de novo* protein synthesis (Supplemental Fig S2c and **S3a**), it is unlikely that the latter mechanism is solely responsible for the observed effect of HDAC inhibition, suggesting that altered transcription of a critical subset of genes is a key component mediating correction.

Given that the activity of HDACi such as SAHA remain challenging to understand, we sought to further identify its relevant *in vivo* target(s). Following a siRNA screen of all class I and II HDACs, we identified HDAC7 as the key target mediating the rescue of ΔF508-CFTR trafficking and restoration of cell surface activity. The mechanism responsible for increased channel activity remains to be investigated and could include alteration in channel gating, recycling or targeting to the lysosome (Fig. 6b).

Intriguingly, the FDA-approved HDACi SAHA8 has previously been shown to decrease the expression of HDAC7[32], an observation which was confirmed in a microarray of SAHA-treated CFBE41o- cells (GM, data not shown). This result reinforces the importance of HDAC7 as the relevant target in the SAHA-mediated rescue of ΔF508. HDAC7 has been implicated in the regulation of both gene expression and protein activity through MEF2 and other transcriptional factors[33,34]. Its activity is controlled by multiple cytoplasmic signaling pathways that regulate its nuclear-cytoplasmic distribution and acetylation-dependent transcriptional responses. Additionally, HDAC7 has been shown to be critical in maintaining the integrity of the vascular endothelial system, yet heterozygous HDAC7 knock-outs exhibit normal endothelial cell integrity33. This suggests normal physiology can tolerate a significant HDAC7 deactivation, making this a viable pharmacological target for correction of ΔF508 function in CF. Although we observed a correction of trafficking with only one other HDAC family member, siHDAC1, we were unable to detect a significant increase in channel activity with a level of knockdown that maintained cell viability, suggesting that HDAC1 sensitive pathways only affect delivery of the channel to the cell surface.

Following treatment of the human lung cell line, CFBE41o-, with HDACi or siHDAC7, a notable transcriptional difference observed was the level of expression of ΔF508, leading to the possibility that this alone might explain the observed increase in cell surface expression of the protein through various mechanisms including saturation of the degradation machinery. However, treatment of primary ΔF/ΔF-HBE cells from patients with SAHA revealed a very modest increase in total CFTR expression in the context of the endogenous CFTR promoter, while observing a significant increase in the appearance of band C and more importantly, the appearance of channel activity (~28% of WT), a level thought to be clinically relevant[35]. This would suggest that the increased expression of CFTR in response to inhibition of HDAC7 is part of a more general HDAC7-regulated set of transcriptional events that restores function. For example, chromatin immunoprecipitation experiments revealed that HDAC7 is found at numerous loci including the Sar1b promoter. Thus, we speculate that an initial step in the mechanism by which HDAC7 may affect the trafficking of stabilized ΔF508-CFTR would be to regulate the level of expression of COPII components available for recruitment of stabilized ΔF508 to ER exit sites, previously shown to be essential for controlling egress of CFTR from the ER (Fig. 6c)[28,29,36].

The potential benefit of inhibiting HDAC7 in correction of CF disease is supported by the effects of HDAC inhibition on reversing other diseases including those involving transcriptional silencing[37-39], normalization of the UPR[11], modulating HSR through SIRT1[14], influencing the inflammatory response12,13, improving the aging environment40 and countering neurodegeneration[41]. 4-phenylbutyrate (4PBA) (**10**) (Supplemental Fig. S1), which is thought to have very weak HDACi activity among many other unknown biological effects given the high concentrations (mM) used to elicit cellular responses, has been shown to promote a modest improvement in human ΔF508 nasal conductance[42-44]. Because 4-PBA is not known to be selective for any particular HDAC, it remains a challenge to interpret the relevant responses enabled by this potential chemical chaperone.

In sum, we have found that reducing the activity of the lung-enriched HDAC7 can trigger altered expression of a subset of CF-interacting gene products and, potentially, unknown factors, to generate a new cellular environment that is both protective and corrective for ΔF508 function (Fig. 6c). Because loss-of-function of CFTR in lung epithelial cells leads to a disease principally impacting tissue physiology, we suggest that HDACi or siHDAC7 could be used to direct a global tissue response to ΔF508 dysfunction that may ultimately improve surface hydration7 and reduce inflammatory responses characteristic of disease[45]. Our data raise the possibility that the tunable capacity of HDAC to modulate the epigenome and other components can be used to manage tissue (patho)physiology to counter the tissue

defects associated with the onset of multiple human loss-of-function misfolding disorders that affect cellular proteostasis[4-6].

SUMMARY OF METHODS

Cell culture and treatment

CFBE41o- expressing ΔF508 or corrected CFBE41o- (WT-HBE41o-) expressing wild-type CFTR were obtained from J.P. Clancy (University of Alabama, Birmingham) and were cultured in α-MEM containing 10% FBS, 2mM L-glutamine and either 2mg/ml puromycin (ΔF508) or 1mg/ml blasticidin (WT). CFBE41o- cells were treated at the indicated concentration of SAHA (Cayman Chemical), TSA (Sigma), Scriptaid (Biomol), MS-275 (Axxora) or vehicle (DMSO) in complete growth media (above). HDAC silencing was performed with RNAiMax (Invitrogen) as per manufacturers protocol using 50nM of the indicated siRNA (Ambion).

Immunoblotting

CFBE41o- cells lysates were prepared in 50mM Tris-HCl, 150mM NaCl, 1% Triton X-100 and 15μg of total protein were separated on an 8% SDS-PAGE. Proteins were transferred to nitrocellulose and probed with M3A7 for CFTR detection or the indicated primary antibodies and appropriate HRP-conjugated secondary antibody and detected by chemiluminescence. CFTR from ΔF/ΔF-HBE cells was detected using antibody #217 from Cystic Fibrosis Foundation Therapuetics.

Cell Surface labeling

Cells surface expression of $\Delta F508^{extope}$ in BHK-21, CFBE41o- or primary HBE cells was detected by HA.11 antibody (Covance) under non-permeabilizing conditions. Detailed protocol and analysis is described in Supplemental Methods

Iodide efflux

CFBE41o- cells were loaded with iodide in cell loading buffer (see Supplemental Methods) for 1h and subsequently washed in iodide free efflux buffer. The iodide content in the extracellular solution was monitored at 1 minute intervals before and after forskolin and genistein stimulation using an iodide selective electrode.

Ussing chamber conductance assay cell culture

CFBE41o- cells stably expressing ΔF508 CFTR and primary ΔF/ΔF-HBE cells were cultured on permeable supports as described previously[46-48]. Short-circuit currents (I_{sc}) were measured as previously described[49,50]

Supplementary Material

Refer to Web version on PubMed Central for supplementary material.

Acknowledgments

Work was supported NIH grants HL56893, GM42336 and the Cystic Fibrosis Consortium (CFC) to WEB; NS055781 to JMG; DK68196, DK72506 and the CFC to RAF; UR98647 and the CFC to ES; AG84567 to JWK; DK23567 to JRR; AG78594 to GM; DK075302 and CHIR to GLL. DMH has received support by fellowships from the Canadian Cystic Fibrosis Foundation and the Canadian Institutes of Health Research; DH was supported by fellowship from the Friedreich's Ataxia Research Alliance. TO was supported by a fellowship from the Canadian Cystic Fibrosis Foundation.

BIBLIOGRAPHY

1. Riordan JR. CFTR function and prospects for therapy. Annu Rev Biochem 2008;77:701–26. [PubMed: 18304008]
2. Qu BH, Strickland EH, Thomas PJ. Localization and suppression of a kinetic defect in cystic fibrosis transmembrane conductance regulator folding. J Biol Chem 1997;272:15739–44. [PubMed: 9188468]
3. Boucher RC. Evidence for airway surface dehydration as the initiating event in CF airway disease. J Intern Med 2007;261:5–16. [PubMed: 17222164]
4. Balch WE, Morimoto RI, Dillin A, Kelly JW. Adapting proteostasis for disease intervention. Science 2008;319:916–9. [PubMed: 18276881]
5. Powers ET, Morimoto RI, Dillin A, Kelly JW, Balch WE. Biological and chemical approaches to diseases of proteostasis deficiency. Annu Rev Biochem 2009;78:959–91. [PubMed: 19298183]
6. Hutt DM, Powers ET, Balch WE. The proteostasis boundary in misfolding diseases of membrane traffic. FEBS Lett 2009;583:2639–46. [PubMed: 19708088]
7. Gregersen N. Protein misfolding disorders: pathogenesis and intervention. J Inherit Metab Dis 2006;29:456–70. [PubMed: 16763918]
8. Marks PA, Breslow R. Dimethyl sulfoxide to vorinostat: development of this histone deacetylase inhibitor as an anticancer drug. Nat Biotechnol 2007;25:84–90. [PubMed: 17211407]
9. Haberland M, Montgomery RL, Olson EN. The many roles of histone deacetylases in development and physiology: implications for disease and therapy. Nat Rev Genet 2009;10:32–42. [PubMed: 19065135]
10. Scroggins BT, et al. An acetylation site in the middle domain of Hsp90 regulates chaperone function. Mol Cell 2007;25:151–9. [PubMed: 17218278]
11. Ozcan U, et al. Chemical chaperones reduce ER stress and restore glucose homeostasis in a mouse model of type 2 diabetes. Science 2006;313:1137–40. [PubMed: 16931765]
12. Adcock IM, Tsaprouni L, Bhavsar P, Ito K. Epigenetic regulation of airway inflammation. Curr Opin Immunol 2007;19:694–700. [PubMed: 17720468]
13. Lin HS, et al. Anti-rheumatic activities of histone deacetylase (HDAC) inhibitors in vivo in collagen-induced arthritis in rodents. Br J Pharmacol 2007;150:862–72. [PubMed: 17325656]
14. Westerheide SD, Anckar J, Stevens SM Jr. Sistonen L, Morimoto RI. Stress-inducible regulation of heat shock factor 1 by the deacetylase SIRT1. Science 2009;323:1063–6. [PubMed: 19229036]
15. Fischle W, et al. Human HDAC7 histone deacetylase activity is associated with HDAC3 in vivo. J Biol Chem 2001;276:35826–35. [PubMed: 11466315]
16. Wang X, et al. Hsp90 cochaperone Aha1 downregulation rescues misfolding of CFTR in cystic fibrosis. Cell 2006;127:803–15. [PubMed: 17110338]
17. Kovacs JJ, et al. HDAC6 regulates Hsp90 acetylation and chaperone-dependent activation of glucocorticoid receptor. Mol Cell 2005;18:601–7. [PubMed: 15916966]
18. Bebok Z, et al. Failure of cAMP agonists to activate rescued deltaF508 CFTR in CFBE41o- airway epithelial monolayers. J Physiol 2005;569:601–15. [PubMed: 16210354]
19. Lukacs GL, et al. Conformational maturation of CFTR but not its mutant counterpart (delta F508) occurs in the endoplasmic reticulum and requires ATP. Embo J 1994;13:6076–86. [PubMed: 7529176]
20. Gentzsch M, et al. Endocytic trafficking routes of wild type and DeltaF508 cystic fibrosis transmembrane conductance regulator. Mol Biol Cell 2004;15:2684–96. [PubMed: 15075371]
21. Lahm A, et al. Unraveling the hidden catalytic activity of vertebrate class IIa histone deacetylases. Proc Natl Acad Sci U S A 2007;104:17335–40. [PubMed: 17956988]
22. Marks PA, Dokmanovic M. Histone deacetylase inhibitors: discovery and development as anticancer agents. Expert Opin Investig Drugs 2005;14:1497–511.
23. Blander G, Guarente L. The Sir2 family of protein deacetylases. Annu Rev Biochem 2004;73:417–35. [PubMed: 15189148]
24. Milne JC, Denu JM. The Sirtuin family: therapeutic targets to treat diseases of aging. Curr Opin Chem Biol. 2008

25. Caci E, et al. Evidence for direct CFTR inhibition by CFTRinh-172 based on arginine 347 mutagenesis. Biochem J. 2008
26. Ekins S, Nikolsky Y, Bugrim A, Kirillov E, Nikolskaya T. Pathway mapping tools for analysis of high content data. Methods Mol Biol 2007;356:319–50. [PubMed: 16988414]
27. Sun F, et al. Derlin-1 promotes the efficient degradation of cystic fibrosis transmembrane conductance regulator (CFTR) and CFTR folding mutants. J. Biol. Chem 2006;281:36856–63. [PubMed: 16954204]
28. Wang X, Koulov AV, Kellner WA, Riordan JR, Balch WE. Chemical and biological folding contribute to temperature-sensitive DeltaF508 CFTR trafficking. Traffic 2008;9:1878–93. [PubMed: 18764821]
29. Wang X, et al. COPII-dependent export of cystic fibrosis transmembrane conductance regulator from the ER uses a di-acidic exit code. J Cell Biol 2004;167:65–74. [PubMed: 15479737]
30. Wiseman RL, Powers ET, Buxbaum JN, Kelly JW, Balch WE. An adaptable standard for protein export from the endoplasmic reticulum. Cell 2007;131:809–21. [PubMed: 18022373]
31. Guggino WB, Stanton BA. New insights into cystic fibrosis: molecular switches that regulate CFTR. Nat Rev Mol Cell Biol 2006;7:426–36. [PubMed: 16723978]
32. Dokmanovic M, et al. Histone deacetylase inhibitors selectively suppress expression of HDAC7. Mol Cancer Ther 2007;6:2525–34. [PubMed: 17876049]
33. Chang S, et al. Histone deacetylase 7 maintains vascular integrity by repressing matrix metalloproteinase 10. Cell 2006;126:321–34. [PubMed: 16873063]
34. Kasler HG, Verdin E. Histone deacetylase 7 functions as a key regulator of genes involved in both positive and negative selection of thymocytes. Mol Cell Biol 2007;27:5184–200. [PubMed: 17470548]
35. Amaral MD. Processing of CFTR: traversing the cellular maze--how much CFTR needs to go through to avoid cystic fibrosis? Pediatr Pulmonol 2005;39:479–91. [PubMed: 15765539]
36. Yoo JS, et al. Non-conventional trafficking of the cystic fibrosis transmembrane conductance regulator through the early secretory pathway. J Biol Chem 2002;277:11401–9. [PubMed: 11799116]
37. Mai A. The therapeutic uses of chromatin-modifying agents. Expert Opin Ther Targets 2007;11:835–51. [PubMed: 17504020]
38. Herman D, et al. Histone deacetylase inhibitors reverse gene silencing in Friedreich's ataxia. Nat Chem Biol 2006;2:551–8. [PubMed: 16921367]
39. Mai A, et al. Identification of two new synthetic histone deacetylase inhibitors that modulate globin gene expression in erythroid cells from healthy donors and patients with thalassemia. Mol Pharmacol 2007;72:1111–23. [PubMed: 17666592]
40. Westphal CH, Dipp MA, Guarente L. A therapeutic role for sirtuins in diseases of aging? Trends Biochem Sci 2007;32:555–60. [PubMed: 17980602]
41. Bates EA, Victor M, Jones AK, Shi Y, Hart AC. Differential contributions of Caenorhabditis elegans histone deacetylases to huntingtin polyglutamine toxicity. J Neurosci 2006;26:2830–8. [PubMed: 16525063]
42. Rubenstein RC, Egan ME, Zeitlin PL. In vitro pharmacologic restoration of CFTR-mediated chloride transport with sodium 4-phenylbutyrate in cystic fibrosis epithelial cells containing delta F508-CFTR. J Clin Invest 1997;100:2457–65. [PubMed: 9366560]
43. Singh OV, et al. Pharmacoproteomics of 4-phenylbutyrate-treated IB3-1 cystic fibrosis bronchial epithelial cells. J Proteome Res 2006;5:562–71. [PubMed: 16512671]
44. Rubenstein RC, Zeitlin PL. A pilot clinical trial of oral sodium 4-phenylbutyrate (Buphenyl) in deltaF508-homozygous cystic fibrosis patients: partial restoration of nasal epithelial CFTR function. Am J Respir Crit Care Med 1998;157:484–90. [PubMed: 9476862]
45. Mroz RM, Noparlik J, Chyczewska E, Braszko JJ, Holownia A. Molecular basis of chronic inflammation in lung diseases: new therapeutic approach. J Physiol Pharmacol 2007;58(Suppl 5): 453–60. [PubMed: 18204158]
46. Lei DC, et al. Episomal expression of wild-type CFTR corrects cAMP-dependent chloride transport in respiratory epithelial cells. Gene Ther 1996;3:427–36. [PubMed: 9156804]

47. Devor DC, Bridges RJ, Pilewski JM. Pharmacological modulation of ion transport across wild-type and DeltaF508 CFTR-expressing human bronchial epithelia. Am J Physiol Cell Physiol 2000;279:C461–79. [PubMed: 10913013]

48. Butterworth MB, Edinger RS, Johnson JP, Frizzell RA. Acute ENaC stimulation by cAMP in a kidney cell line is mediated by exocytic insertion from a recycling channel pool. J Gen Physiol 2005;125:81–101. [PubMed: 15623897]

49. Myerburg MM, et al. Airway surface liquid volume regulates ENaC by altering the serine protease-protease inhibitor balance: a mechanism for sodium hyperabsorption in cystic fibrosis. J Biol Chem 2006;281:27942–9. [PubMed: 16873367]

50. Myerburg MM, et al. Prostasin expression is regulated by airway surface liquid volume and is increased in cystic fibrosis. Am J Physiol Lung Cell Mol Physiol 2008;294:L932–41. [PubMed: 18310226]

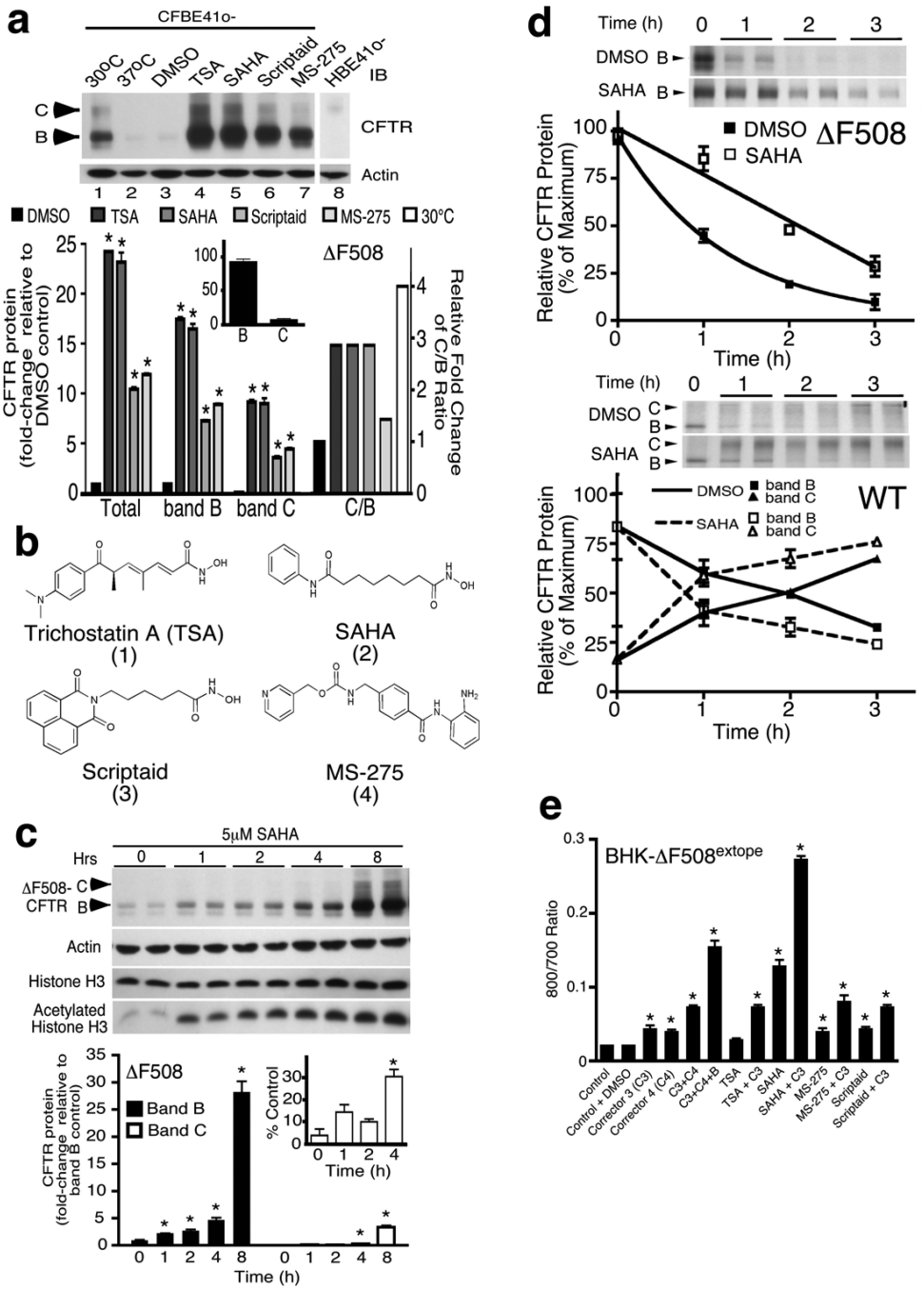

Fig. 1. HDAC inhibitor treatment increases ΔF508-CFTR expression and trafficking

a, Immunoblot analysis (upper) and quantitation (lower) of CFTR expression following treatment of CFBE41o- cells with 0.1 μM TSA, 5 μM SAHA, 1 μM Scriptaid and 5 μM MS-275. Data are presented as fold change relative to vehicle treatment (mean ± SEM, n ≥ 3) (inset: levels for vehicle treated control). C/B ratio expressed as a fold change relative to vehicle treatment. **b**, Chemical structure of HDACi tested in **a**. **c,** Immunoblot analysis (upper) of CFTR and histone H3 expression and CFTR quantitation (lower) following treatment of CFBE41o- cells with 5 μM SAHA for the indicated time (inset: band C analysis for the first 4 h). Data shown as a percent of band B in vehicle treatment (mean ± SD, n = 2). **d**, Pulse chase analysis of ΔF508-CFTR (upper) and wild-type CFTR (lower) following

treatment of cells with 5 μM SAHA for 24 h. Data shown as percent of maximum CFTR at t = 0 (mean ± SD, n = 2). **e**, Surface expression of $\Delta F508^{extope}$ in BHK cells following treatment with 0.02% DMSO, 25 μM of correctors C3, C4 (**11**) and 4-PBA (B) (**12**), 0.1 μM TSA, 5 μM SAHA, 1 μM Scriptaid or 5 μM MS-275 or combinations with C3. (mean ± SEM, n=3). In all panels, asterisk indicates significant differences ($p < 0.05$) relative to DMSO treatment as determined by two-tailed t-test.

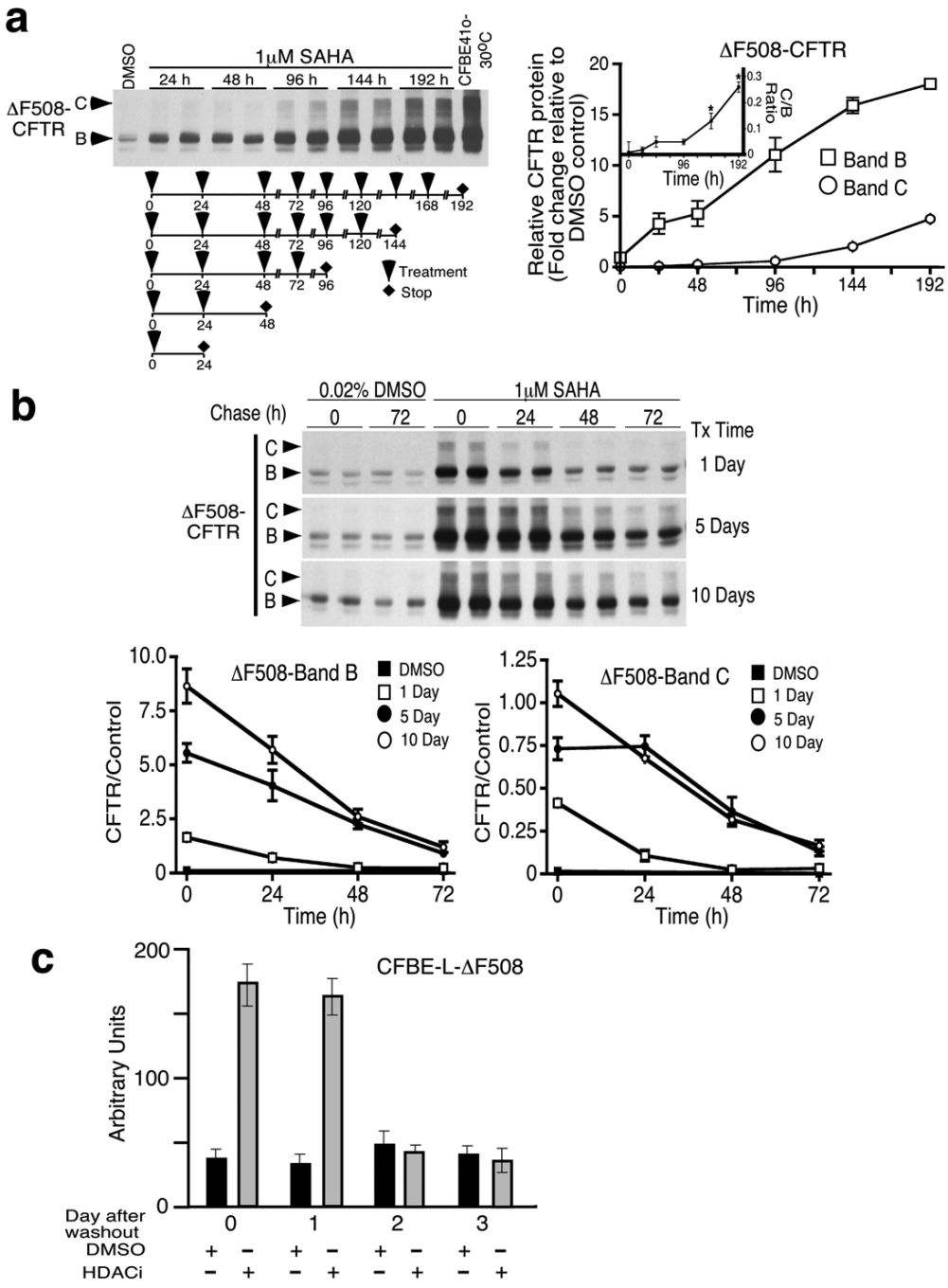

Fig. 2. Low dose SAHA treatment increases ΔF508-CFTR stability and trafficking

a, (Left panel) Immunoblot analysis of ΔF508 following chronic application of 1 μM SAHA to CFBE41o- cells for the indicated time. The treatment schema is shown beneath the immunoblot. (Right panel) Quantitation of the different glycoforms and the C/B ratio (inset) are shown. Data shown as fold change relative to vehicle treatment (mean ± SEM, n=4). **b**, (Upper) Immunoblot analysis of ΔF508 following chronic application of 1 μM SAHA to CFBE41o- cells following treatment for 1, 5 and 10 days and subsequent washout. The lower panels show quantitation of bands B and C. The data shown as a ratio of CFTR glycoform at the indicated time relative to the level of band B in the control condition (mean ± SEM; n = 4). **c,** Cell surface density of extracellular epitope-tagged ΔF508 stably

expressed in CFBE41o- cells (CFBE-L-ΔF508) following pretreatment for 5 days and indicated washout (mean ± SEM, n=8). In all panels, asterisk indicates significant differences ($p < 0.05$) relative to DMSO treatment as determined by two-tailed t-test.

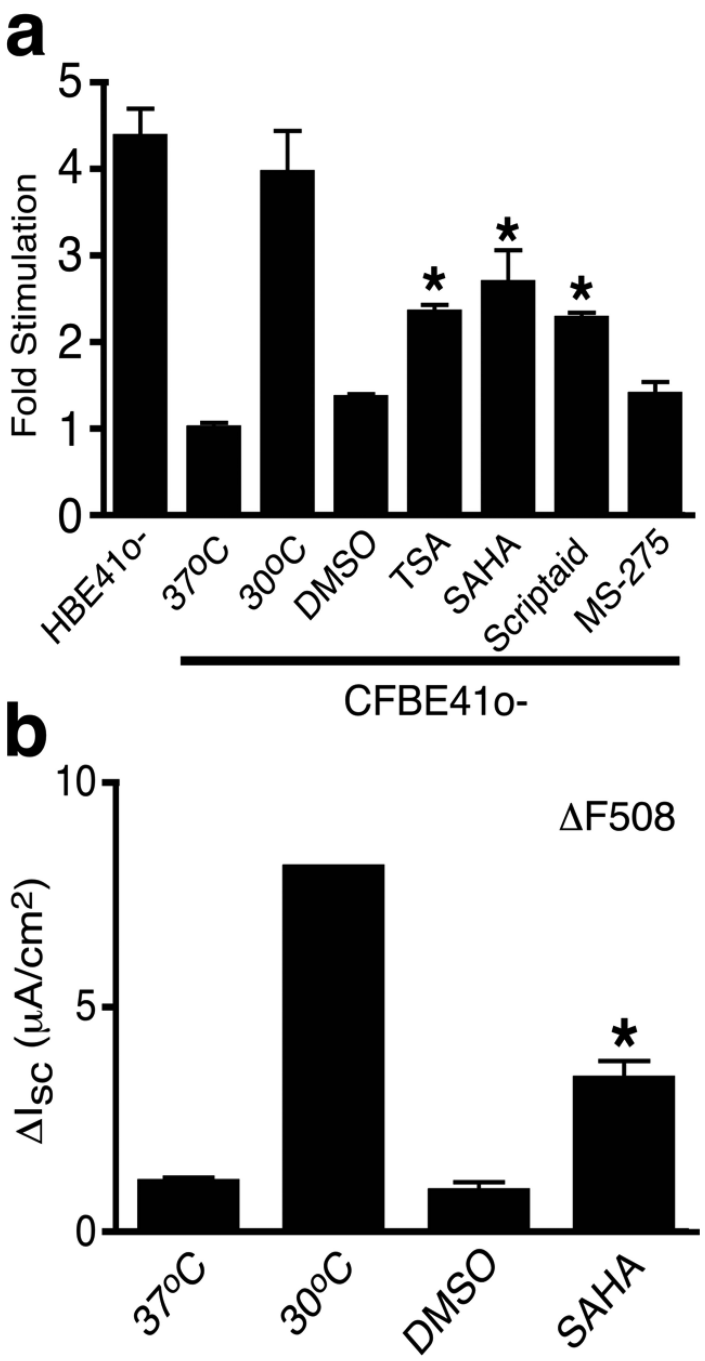

Fig. 3. HDAC inhibitor treatment activates ΔF508 channel activity

a, The effect of 0.1 μM TSA, 5 μM SAHA, 1 μM Scriptaid, 5 μM MS-275 (24 h at 37°C) on the fold-change in cAMP-mediated iodide efflux relative to the non-treated CFBE41o- cells (mean ± SEM; n ≥ 3). **b**, Difference in transepithelial short-circuit currents (ΔI_{sc}) in response to Fsk, Fsk + Gst and CFTRinh-172 following treatment of CFBE41o- monolayers at reduced temperature (30°C) or with 10 μM SAHA for 24 h (mean ± SEM; n > 6). In all panels, asterisk indicates significant differences ($p < 0.05$) relative to DMSO treatment as determined by two-tailed t-test.

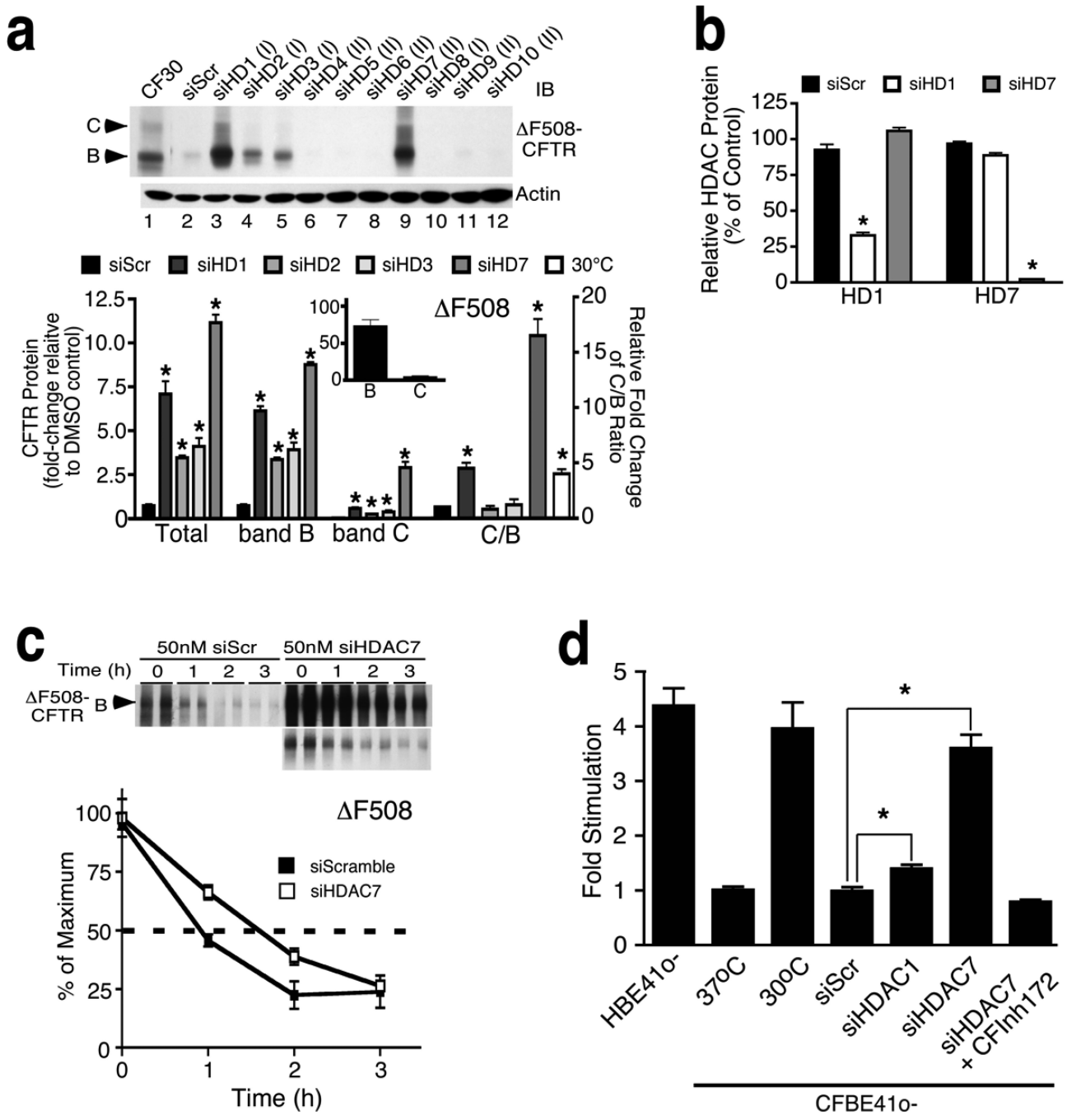

Fig. 4. Silencing of HDAC7 increases ΔF508-CFTR expression, trafficking and activity

a, (Upper panel) Immunoblot analysis of CFTR following siRNA-mediated HDAC silencing in CFBE41o- cells. (Lower panel) quantitative analysis of total CFTR, glycoforms and C/B ratio following silencing of HDACs 1, 2, 3 and 7. Data are expressed as fold change relative to siScr control (mean ± SEM; n=3). The inset represents the glycoform levels for siScr control samples. **b**, Analysis of HDAC1 and HDAC7 protein levels following their respective silencing in CFBE41o- cells (mean ± SEM; n=3). **c**, Pulse-chase of CFTR after HDAC7 silencing in CFBE41o- cells. Quantitation of CFTR band B glycoform levels is presented as the percentage of maximal CFTR seen at t = 0. (mean ± SEM; n = 3). **d,** The effect of siHDAC1 and siHDAC7 on the fold-change in cAMP-mediated iodide efflux

relative to the non-treated CFBE41o- cells (mean ± SEM; n ≥ 3). In all panels, asterisk indicates significant differences ($p < 0.05$) relative to siScr treatment as determined by two-tailed t-test.

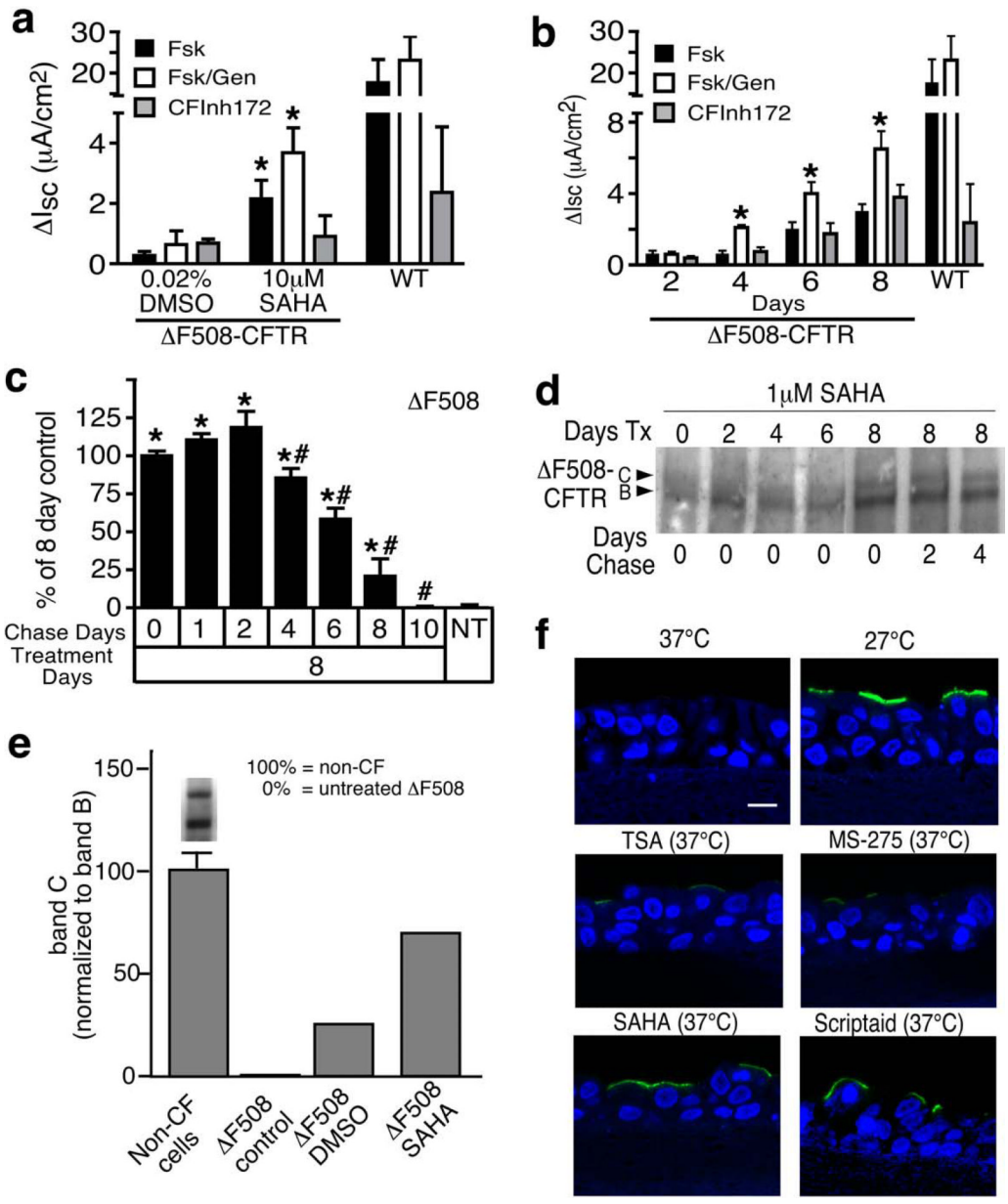

Fig. 5. SAHA rescues ΔF508-CFTR activity in primary human bronchial epithelial cells

a, ΔI_{SC} in response to Fsk, Fsk + Gst and CFTRinh-172 following treatment of ΔF/ΔF-HBE with 10 μM SAHA or DMSO. Asterisk indicates a significant change ($p \leq 0.05$) relative to vehicle treatment. **b**, ΔI_{SC} as in **a,** following treatment of ΔF/ΔF-HBE with 1 μM SAHA for the indicated time. Asterisk indicates a significant change ($p \leq 0.05$) relative to 2-day treatment. **c**, ΔI_{SC} as in **a,** following treatment of ΔF/ΔF-HBE with 1 μM SAHA and washout for the indicated time. Asterisk and # indicate a significant change ($p \leq 0.05$) relative to non-treatment (NT),and 8 days without washout (8 day + 0) respectively. Data shown as a percent of 8 day + 0. **d**, CFTR immunoblot of ΔF/ΔF-HBE lysates following treatment with 1 μM SAHA for the indicated treatment and washout time. **e**, CFTR band C analysis in non-CF HBE, ΔF/ΔF-HBE and ΔF/ΔF-HBE treated with 0.02% DMSO or 10 μM SAHA. Inset depicts non-CF HBE lysates. Data shown as ratio of band C to actin and the non-CF HBE ratio normalized to 100% (mean ± SEM; n = 3). **f,** Representative images depicting the

effect of 0.1 μM TSA, 5 μM SAHA, 5 μM MS-275 and 1 μM Scriptaid on the localization of $\Delta F508^{extope}$ in primary HBE cells (scale bar = 10 μM). In panels **a-c** data is mean ± SEM, n > 6. In all panels, p values determined by two-tailed t-test between compared data points.

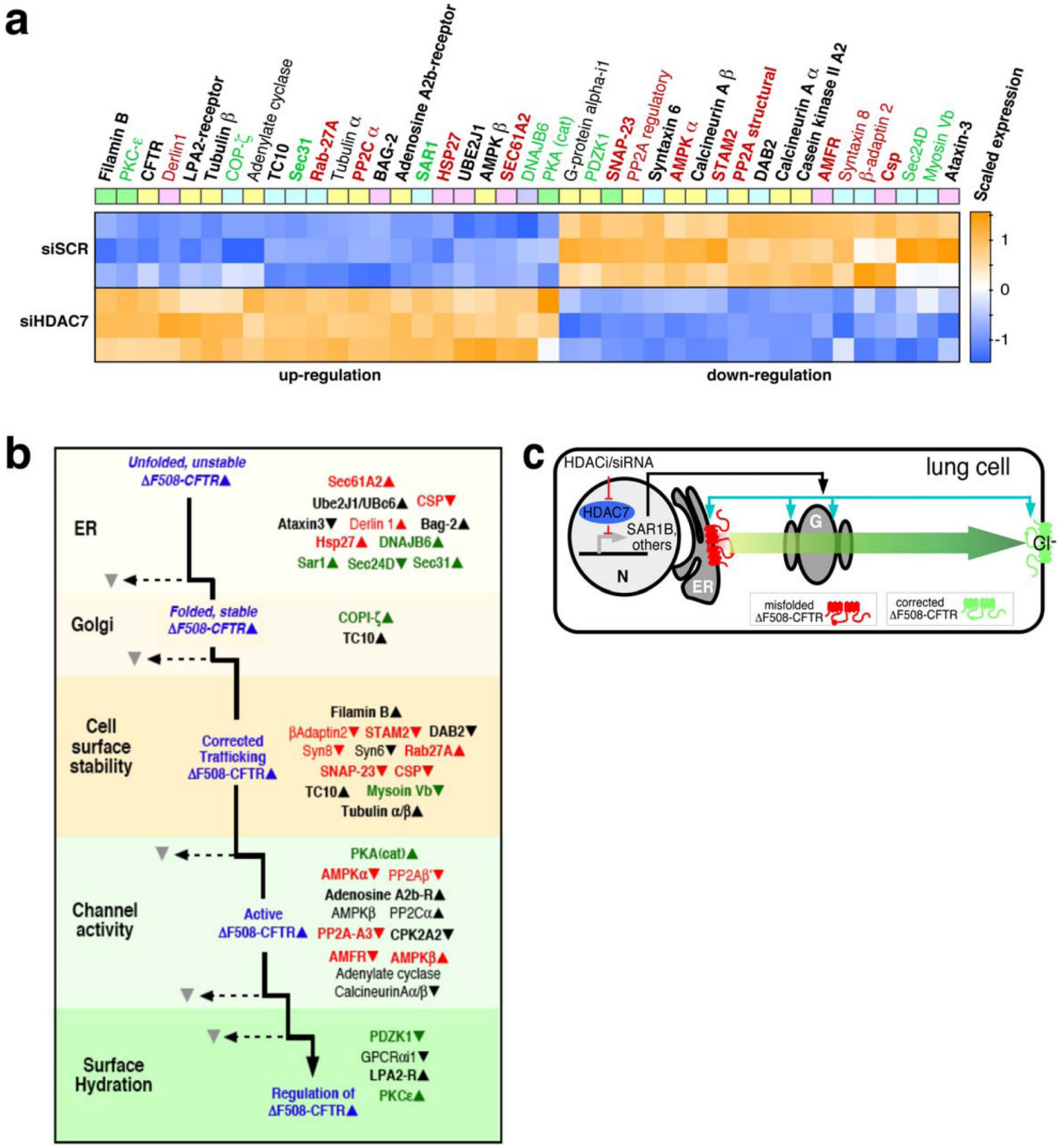

Fig. 6. Mechanism of HDAC7-mediated ΔF508 multi-target pathway correction

a, Clustered display of the preprocessed expression matrix, showing probeset-scaled expression values (adjusted p-value<0.01) following siHDAC7 treatment of CFBE41o-cells. In all panels, the color gradient goes from blue (low) to orange (high). The reported biological effect on CFTR of indicated proteins is coded as follows: red: negatively affect CFTR stability, trafficking and/or activity; green: positively affect CFTR stability, trafficking and/or activity; black: unknown effects. Bold typeface indicates an increased expression change greater then 2-fold. Functional assignments based on the CF pathways platform are depicted in colored boxes to the left of the gene name with the key code depicted in Supplemental Fig. S7. **b**, Cartoon depicting potential steps in a pathway of

HDAC7-based correction. The diagram illustrates a branched pathway in which the observed alteration in the transcriptional environment (colored arrowhead indicating up- or down-regulation in **a**) affects the stability, trafficking and/or activity of ΔF508. Bold solid lines represent steps favoring positive effect on correction of function while dotted lines represent steps leading to loss of function. **c**, Hypothetical model by which the HDAC7-sensitive transcriptional regulation of CFTR interacting genes leads to correction of the ΔF508 trafficking defect.